ISSN 0020-1685, Inorganic Materials, 2020, Vol. 56, No. 2, pp. 142–150. © Pleiades Publishing, Ltd., 2020.
Russian Text © The Author(s), 2020, published in Neorganicheskie Materialy, 2020, Vol. 56, No. 2, pp. 151–159.

Self-Propagating High-Temperature Synthesis of $MgAl_2O_4$ Spinel

N. I. Radishevskaya[a], A. Yu. Nazarova[a, *], O. V. L'vov[a], N. G. Kasatskii[a], V. G. Salamatov[b], I. V. Saikov[b], and D. Yu. Kovalev[b]

[a] *Tomsk Scientific Center, Siberian Branch, Russian Academy of Sciences, Akademicheskii pr. 10/4, Tomsk, 634055 Russia*

[b] *Merzhanov Institute of Structural Macrokinetics and Materials Science, Russian Academy of Sciences, ul. Akademika Osip'yana 8, Chernogolovka, Moscow oblast, 142432 Russia*

**e-mail: osm.nazarova@yandex.ru*

Received February 15, 2019; revised July 1, 2019; accepted July 11, 2019

Abstract—Magnesium aluminate spinel, $MgAl_2O_4$, has been prepared by self-propagating high-temperature synthesis (SHS) in the $MgO–Al_2O_3–Mg(NO_3)_2 \cdot 6H_2O–Al–B$ system. The composition and structure of the synthesis product have been ascertained by X-ray diffraction, infrared spectroscopy, and scanning electron microscopy. Using time-resolved X-ray diffraction (TRXRD), we have studied the phase formation process during SHS and identified the key reaction paths. The addition of 2–4 wt % boron has been shown to result in the formation of a liquid phase during the combustion process owing to the formation of a low-melting-point boron oxide, favoring the growth of skeletal spinel crystals 1–10 μm in size. Our results demonstrate that the use of a mixture of aluminum and boron as combustible components of the starting mixture and heating at a rate above 100°C/min allow a material containing more than 95 wt % $MgAl_2O_4$ spinel to be obtained.

Keywords: self-propagating high-temperature synthesis, time-resolved X-ray diffraction, spinel, sequential and parallel reactions

DOI: 10.1134/S0020168520010112

INTRODUCTION

$MgAl_2O_4$ spinel is an excellent refractory material chemically stable in mineral acids. It has good dielectric properties and its hardness is 7.5–8 on Mohs' scale. The melting pint of $MgAl_2O_4$ is 2135°C, which allows it to be thought of as a refractory ceramic material capable of operating in aggressive media at temperatures up to 1500–1750°C [1, 2]. Artificially synthesized spinel-based engineering ceramics are used in radio and electrical engineering, electronics, chemical engineering, and other application fields. Natural and synthetic transparent colored spinel varieties are used as gemstones. Spinel finds application as a catalyst and in the manufacture of durable ceramic pigments [3–5].

Spinel is typically synthesized by reaction sintering of its constituent oxides at a temperature of at least 1200°C or by a sol–gel process followed by annealing, which is due to large energy consumption [1, 6].

Self-propagating high-temperature synthesis (SHS) is a promising, energy-saving process for the preparation of magnesium aluminate spinel. Aluminum is widely used as a reducing agent in SHS. The large energy release during aluminum oxidation and its relative availability and low cost make Al an attractive for use in these processes. Another reducing agent having a large heat of combustion and employed in solid fuel is boron. Some physicochemical properties of aluminum and boron are indicated in Table 1 [7–9].

The chemical paths of self-sustaining exothermic reactions and $MgAl_2O_4$ spinel combustion and structure formation mechanisms in systems containing Al and B as reducing agents remain unexplored.

The purpose of this work is to study the sequence of chemical reactions and their effect on the structure formation and phase composition of reaction products in the SHS of $MgAl_2O_4$ spinel in the $MgO–Al_2O_3–Mg(NO_3)_2 \cdot 6H_2O–Al–B$ system.

EXPERIMENTAL

The starting chemicals used were pure-grade magnesium oxide (MgO) and aluminum oxide (Al_2O_3) powders, ASD-4 aluminum powder with a particle size under 30 μm, amorphous boron powder (B 99A, Russian Federation Purity Standard TU 6-02-585-75) with a particle size from 1 to 5 μm, and reagent-grade magnesium nitrate hexahydrate ($Mg(NO_3)_2 \cdot 6H_2O$). The composition of the $MgO + Al_2O_3 + Mg(NO_3)_2 \cdot 6H_2O + Al$ starting mixture corresponded to the $MgAl_2O_4$ stoichiometry. To the starting mixture, we added 2 or 4 wt % boron and 7.4 or 7.3 wt % aluminum, respectively. The powder mixture was pressed

Table 1. Physicochemical properties of aluminum, boron, and their oxides

Substance	ρ, g/cm^3	t_m, °C	t_b, °C	Q_H, kJ/kg	$-\Delta H^\circ_{298}$, kJ/mol
Al	2.699	660	2500	31033	0
B	2.34	2075	3700	58113	0
Al_2O_3	3.96	2050	2980	–	1676
B_2O_3	1.84	450	2043	–	1254

Q_H is the heat of combustion.

into bars 13 × 10 × 5 mm in dimensions, with a relative density of 0.65.

The phase formation mechanism was studied by time-resolved X-ray diffraction (TRXRD), a method that allows changes in the phase composition of materials to be followed in real time [10]. Data were obtained using CuK_α radiation (λ = 1.54187 Å). A sample was placed in a resistance furnace having X-ray transparent windows. The primary beam was incident on the central part of the sample surface at an angle of ~20° and illuminated an area 2 × 10 mm^2 in dimensions. X-ray diffraction photographs were obtained in the angular range 2θ = 25°–62°. The exposure time per X-ray diffraction photograph was 4 s, and the number of photographs in a series was 64. In a number of cases, just before the instant of ignition, the exposure time was 1 s. The temperature was monitored with a Chromel–Alumel thermocouple, with its junction located in the central part of the sample at a depth of 2 mm. The thermocouple signal was fed to an analogue–digital converter and then recorded at a frequency of 250 Hz. The signal was synchronized with the instant at which we began to record the diffraction pattern of the process. The samples were placed on a BN substrate in the furnace. The heating rate was 7–10 and 130–140°C/min. After ignition of the samples, external heating by the furnace was switched off. The synthesis process was run in air.

After cooling, the phase composition of the synthesis products was determined by X-ray diffraction on a DRON-3M diffractometer. Intensity data were collected in step scan mode with CuK_α radiation in the angular range 2θ = 7°–70° with a scan step of 0.02° and counting time per data point of 2 s. Quantitative phase analysis was carried out by the Rietveld profile analysis method with PDWin 6.0 software. In our calculations, we refined the diffraction line profile parameters, background, thermal factors, the unit-cell parameters of the crystals, and the percentages of the phases present. The weighted profile agreement factor R_{wp} was 10–12%.

Structural features were studied by infrared spectroscopy on a Nicolet 5700 Fourier transform IR spectrometer using KBr pellets. The microstructure of the samples was examined by scanning electron microscopy (SEM) on a Philips SEM 515.

RESULTS AND DISCUSSION

Heating a sample to a critical temperature led to self-ignition. Combustion occurred in the thermal explosion regime. The data in Table 2 illustrate the effect of heating rate on the ignition temperature of the samples, the maximum synthesis temperature, and the phase composition of the synthesis products. It is seen that the heating rate of the samples has a significant effect on the staging of the processes involved and the content of the desired product, $MgAl_2O_4$ spinel. Only rapid heating ensures the preparation of an essentially single-phase product (Fig. 1a). In the case of slow heating, ignition begins at higher temperatures, the maximum synthesis temperature does not exceed 1000°C, and the final product consists of several phases, including the starting mixture components: Al_2O_3 and MgO (Fig. 1b).

Figure 2 presents typical X-ray diffraction data illustrating the process during slow heating of the mixture containing 4 wt % B. A sequence of X-ray diffraction photographs is represented as a two-dimensional field in the (angle, time) plane, where the intensity of the lines is proportional to the gray-scale level. During the first 58 min of heating, the exposure time per X-ray diffraction photograph was 4 s. After 450°C was reached, the exposure time was reduced to 1 s in order to resolve details of the process (Fig. 2b). The light horizontal bands in the diffraction field are due to the limited number of X-ray diffraction photographs obtained in each series: 64. The time needed to digitize the data obtained in one series and then again turn on the data acquisition system was at least 12 s. Superimposed on the total diffraction field is the synchronously recorded heating curve.

It is worth noting that the X-ray diffraction pattern of the starting mixture showed reflections from not only the starting compounds but also an unknown phase. The X-ray diffraction pattern contained strong diffraction lines whose position differed from that for known compounds in the system under consideration, data for which are presented in the ICDD database for polycrystals and the ICSD database for inorganic single crystals. Given that the starting mixture contained a reducing agent (B) and oxidant ($Mg(NO_3)_2 \cdot 6H_2O$), mixing could lead to the formation of a hydrous compound consisting of Mg, N, O, H, and B and missing

Table 2. Effect of the heating rate on the synthesis temperature of $MgAl_2O_4$ spinel and final reaction products

Heating rate , °C/min	8 (slow heating of the starting mixture)		135 (rapid heating of the starting mixture)	
wt % B	2	4	2	4
t_0, °C	590	500	400	400
t_{max}, °C	950	750	1150	1020
Phase composition of the synthesis products	$MgAl_2O_4$*, Al_2O_3, MgO, Al, $2MgO \cdot B_2O_3$, $3MgO \cdot B_2O_3$	$MgAl_2O_4$*, Al_2O_3, MgO, Al, $2MgO \cdot B_2O_3$, $3Al_2O_3 \cdot B_2O_3$	93.8% $MgAl_2O_4$, 1.4% α-BN, 4.8% α-Al_2O_3	95.6% $MgAl_2O_4$, 4.1% α-BN

t_0 and t_{max} are the onset and maximum temperatures of SHS.
* Major phase.

in the powder diffraction databases. According to the TRXRD data, the diffraction lines of the unidentified phase disappear at a temperature above 120°C.

Analysis of the diffraction data in Fig. 2 indicates that, in the case of slow heating, the lines of Al_2O_3 and MgO are observed throughout the heating–ignition–cooling cycle. At temperatures above 325°C, the intensity of the line of MgO considerably increases, suggesting that its content in the mixture increases as a result of magnesium nitrate decomposition:

$$2Mg(NO_3)_2 \cdot 6H_2O = 2MgO + 4NO_2 + O_2 + 12H_2O. \quad (1)$$

In addition, starting at 125°C we observe an increase in the intensity of the lines of Al_2O_3. It is reasonable to assume that this is due to partial oxidation of aluminum. SEM data (Fig. 3) confirm that, after heating to a temperature of 500°C, the surface of the Al particles is covered with an oxide layer. The low temperature of the onset of oxide layer growth on the surface of the Al particles is probably due to the active oxidizing gaseous atmosphere resulting from $Mg(NO_3)_2 \cdot 6H_2O$ decomposition.

The diffraction lines of Al are observed throughout heating, until the ignition of the sample (Fig. 2). With increasing temperature, their intensity decreases and

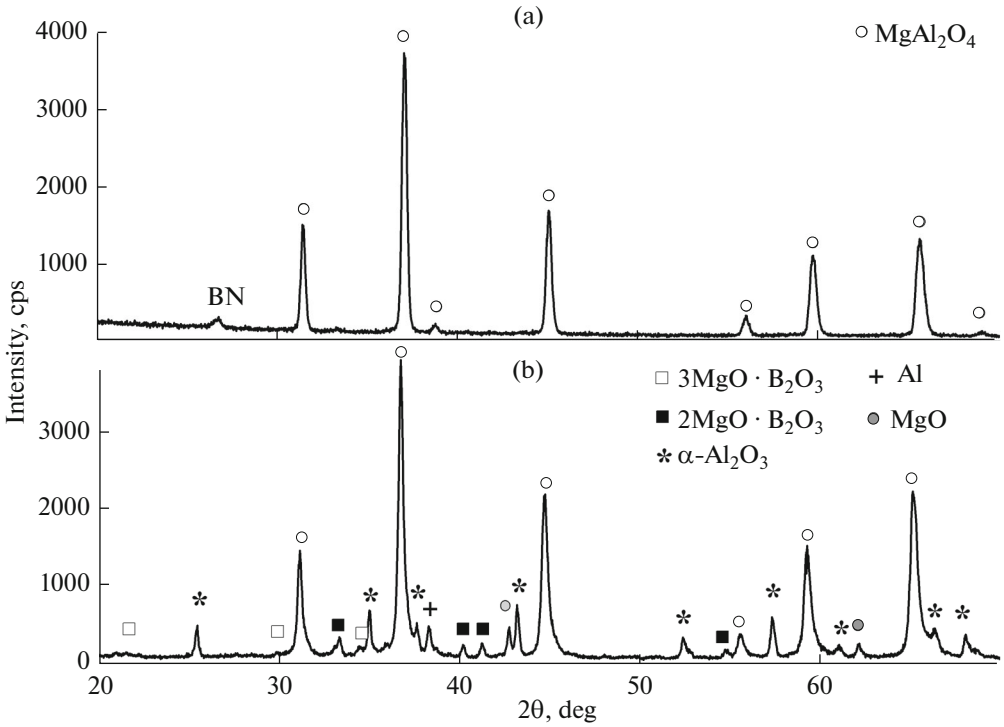

Fig. 1. X-ray diffraction patterns of the combustion products of a $MgO + Al_2O_3 + Mg(NO_3)_2 \cdot 6H_2O + Al + 4\%$ B mixture: (a) rapid and (b) slow heating.

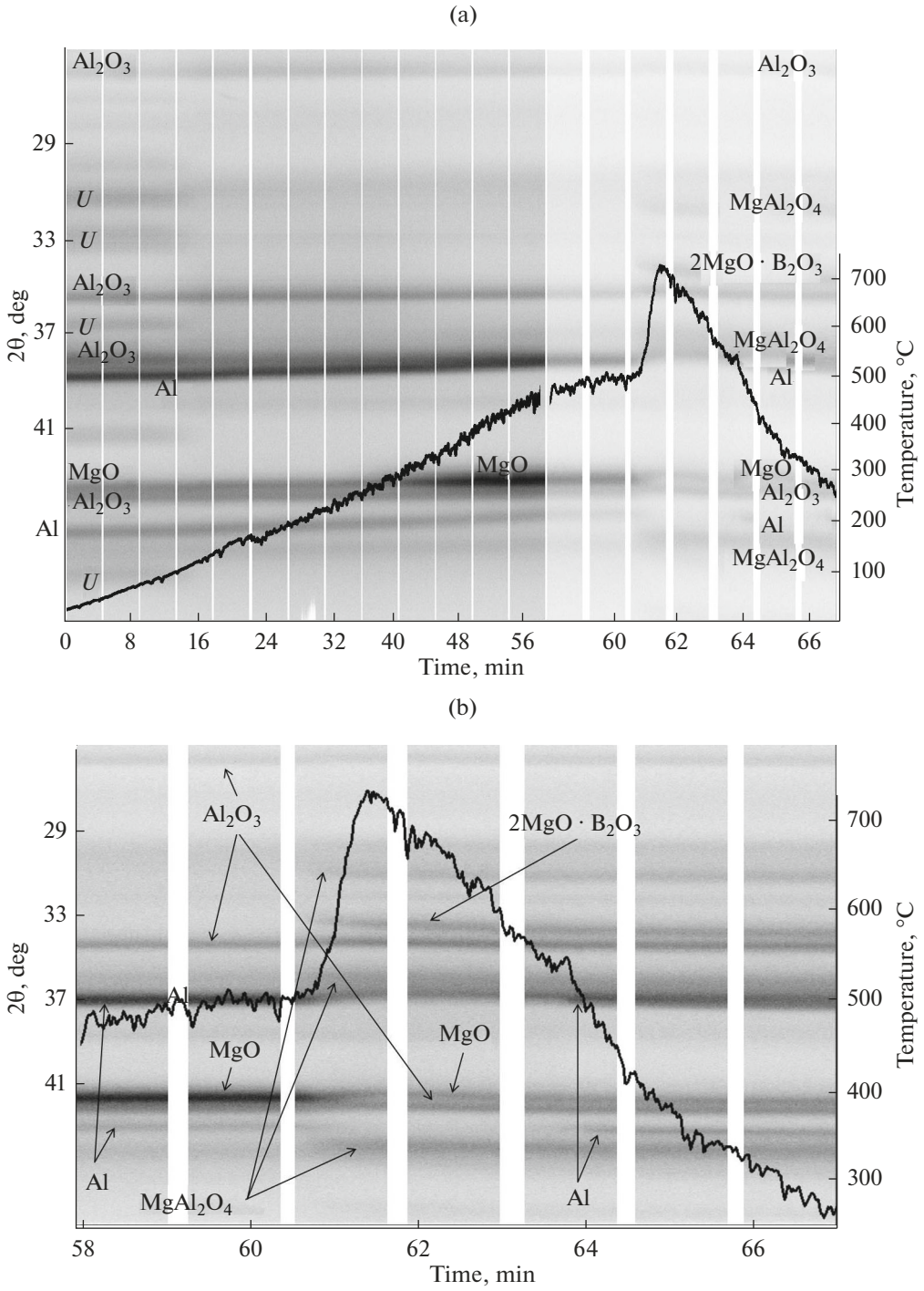

Fig. 2. X-ray diffraction data obtained during slow heating of a $MgO + Al_2O_3 + Mg(NO_3)_2 \cdot 6H_2O + Al + 4\%$ B mixture: (a) total sequence of 1280 X-ray diffraction photographs; (b) sequence of 448 photographs with an exposure time of 1 s before ignition of the sample (*U* marks the unidentified lines).

they shift to smaller angles as a result of thermal extension. The mixtures containing 2 and 4 wt % boron ignite at temperatures of 590 and 500°C, respectively. The amount of boron had no significant effect on the diffraction patterns of the combustion of the mixtures containing different amounts of boron. After ignition, the lines of Al disappear from the diffraction field, but after cooling to below the melting point of aluminum they emerge again. After ignition, the mixture is heated to temperatures no higher than 1000°C. As a result, strong lines of $MgAl_2O_4$ spinel and $2MgO \cdot B_2O_3$ emerge in the diffraction field. It is reasonable to

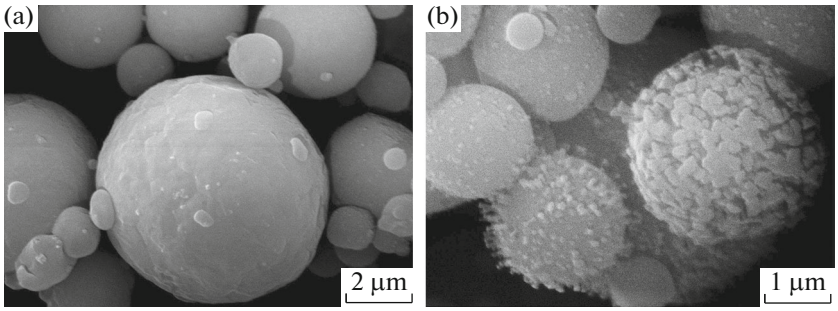

Fig. 3. Micrographs of ASD-4 aluminum particles (a) before and (b) after heating to 500°C.

assume that the rise in temperature is predominantly due to amorphous boron oxidation reaction. The heat of combustion of boron is almost twice that of aluminum (Table 1). The B_2O_3 formed (t_m = 480°C) is in a liquid state at temperatures above 500°C and reacts with magnesium oxide to form magnesium borate, $2MgO \cdot B_2O_3$. Raising the temperature of the mixture leads to reaction between magnesium and aluminum oxides and spinel formation:

$$4B + 3O_2 = 2B_2O_3, \quad (2)$$

$$2MgO + B_2O_3 = 2MgO \cdot B_2O_3, \quad (3)$$

$$MgO + Al_2O_3 = MgAl_2O_4. \quad (4)$$

The X-ray diffraction data for the combustion product obtained during slow heating (Fig. 2b) demonstrate that $MgAl_2O_4$ spinel is a major phase. At the same time, the material contains the starting phases Al_2O_3, MgO, and Al and the magnesium borates $2MgO \cdot B_2O_3$ and $3MgO \cdot B_2O_3$.

To confirm the above assumptions, we carried out an experiment in which the sample containing 2 wt % B was slowly heated to 580°C and then cooled, without ignition. X-ray diffraction characterization of the sample after cooling (Fig. 4) showed that the resultant material contained no oxidant ($2Mg(NO_3)_2 \cdot 6H_2O$) and that the MgO content exceeded that of the starting mixture. Attention should be paid to the fact that the X-ray diffraction pattern of this sample contains a halo, as distinct from that of the starting mixture, which obviously indicates that the material contains an X-ray amorphous B_2O_3 phase. Therefore, in the case of slow heating, a single-phase desired product, $MgAl_2O_4$, cannot be obtained.

The X-ray diffraction data for the process caused by rapid heating of the mixture under study differ significantly from those above. Figure 5 shows a sequence of 64 X-ray diffraction photographs characterizing the process caused by heating the MgO + Al_2O_3 + $Mg(NO_3)_2 \cdot 6H_2O$ + Al mixture containing 4 wt % B at an average rate of 135°C/min until the instant of ignition. The exposure time per X-ray diffraction photograph was 2 s.

Analysis of the X-ray diffraction data in Fig. 5 shows that the lines of the starting mixture components Al_2O_3, MgO, and Al persist until the ignition of the sample. The thermal explosion of the mixtures containing 2 and 4 wt % boron occurs at a temperature near 400°C. The amount of boron has no effect on the diffraction data for combustion of the mixtures. The lines of the unidentified compound formed during mixing of the starting powders and those of the $Mg(NO_3)_2 \cdot 6H_2O$ oxidant disappear from the diffraction photograph at a temperature near 250°C. Clearly, this is due to the decomposition of the phases based on crystalline magnesium nitrate hydrates according to the overall reaction scheme (1). Like in the case of slow heating, after the dissociation of $Mg(NO_3)_2 \cdot 6H_2O$ and the unidentified compound the intensity of the lines of Al_2O_3 increases. At a temperature above 325°C, we observe a marked increase in the intensity of the lines of the starting phase MgO, which is due to the formation of additional MgO as a result of magnesium nitrate decomposition. After thermal explosion, the diffraction lines of all the starting mixture components disappear from the diffraction photograph in 2 s. After ignition, the temperature rises sharply to 1050–1150°C, depending on the boron content of the mixture. As a result, the diffraction photograph shows strong lines of $MgAl_2O_4$ spinel (Fig. 5), which are markedly broadened because, after ignition, the sample surface deflects from the reflection angle. There are no diffraction lines of any other phases. Heat release in the system under investigation seems to be mainly due to boron oxidation.

Amorphous boron is known to ignite between 640 and 800°C and burn with a bright flame, but the resulting B_2O_3 film prevents it from complete combustion. In an oxidizing medium or water vapor, boron can ignite at a temperature as low as 327°C [11]. According to other reports, ignition of fine-particle (≤1 μm) boron in a humid atmosphere occurs at an initial temperature from 230 to 530°C [12]. Magnesium nitrate decomposition is accompanied by the release of the water of crystallization, nitrogen oxides, and oxygen. In the case of rapid heating, the forming gases and water vapor have no time to escape from the

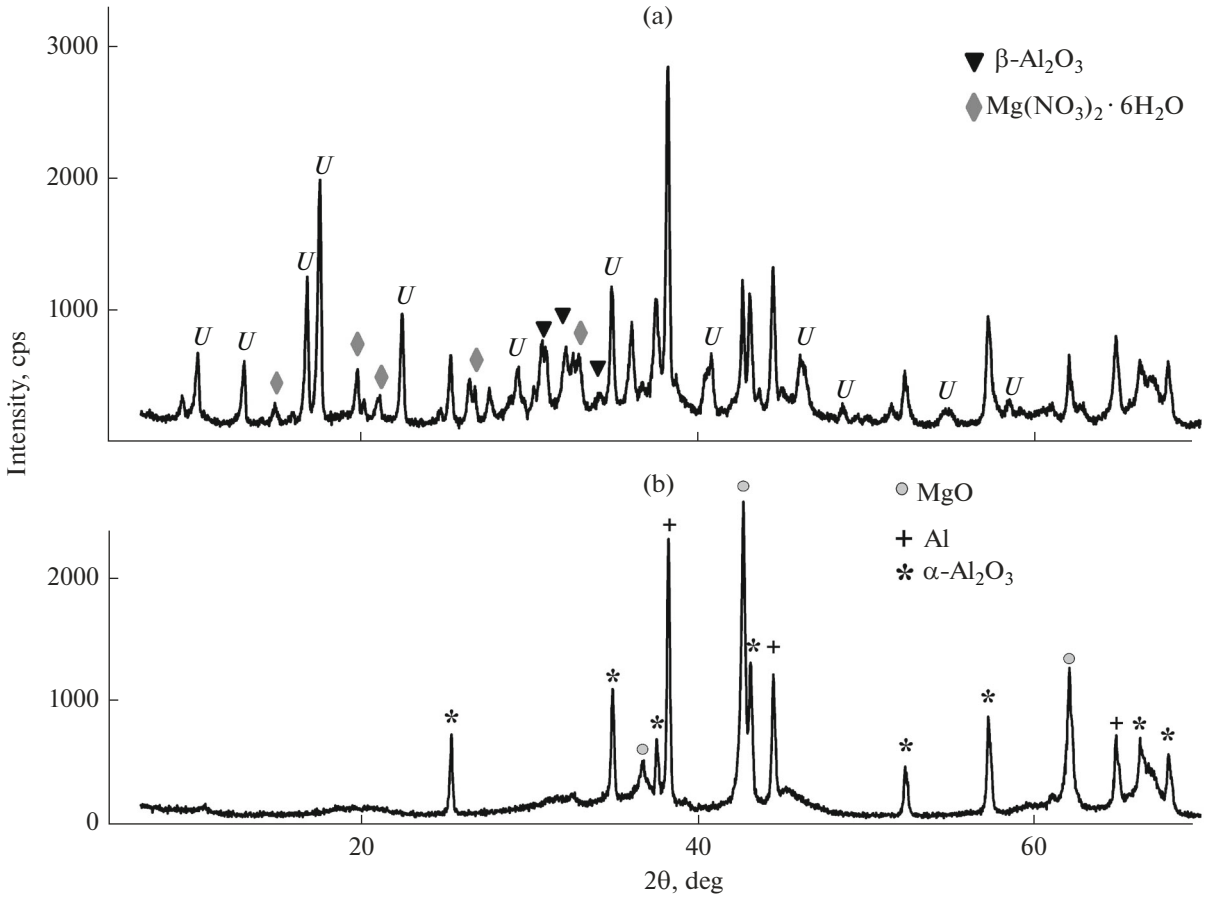

Fig. 4. X-ray diffraction patterns of the $MgO + Al_2O_3 + Mg(NO_3)_2 \cdot 6H_2O + Al$ mixture containing 2 wt % B: (a) initial state, (b) after heating to 580°C without ignition (*U* marks the unidentified lines).

sample to the atmosphere. Boron oxidation is due to not only reaction (2) but also interaction with water vapor:

$$3H_2O(\text{vapor}) + 2B = B_2O_3 + 3H_2\uparrow. \quad (5)$$

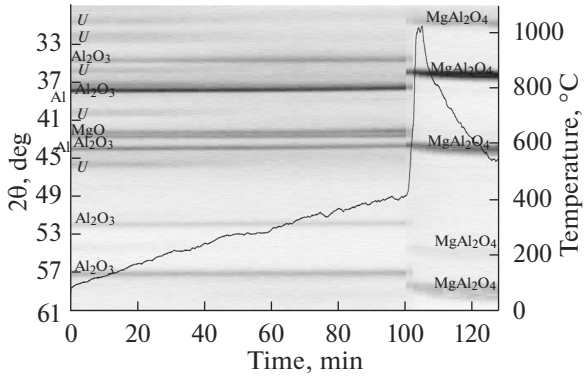

Fig. 5. Diffraction data for the $MgO + Al_2O_3 + Mg(NO_3)_2 \cdot 6H_2O + Al + 4\%$ B mixture during rapid heating.

Moreover, rapid heating causes cracking of the oxide film on the aluminum surface, ensuring more complete oxidation of the aluminum [11]. The mixture of nitrogen oxides resulting from magnesium nitrate hexahydrate decomposition is an oxidizing, highly reactive medium. NO_2 is known to decompose at temperatures from 135 to 620°C to give nitric oxide and oxygen [13]:

$$2NO_2 = 2NO + O_2. \quad (6)$$

The presence of nitrogen oxides can initiate the reaction [13]

$$5B + 3NO = 3BN + B_2O_3. \quad (7)$$

Quantitative X-ray diffraction data demonstrate that the material obtained during rapid heating of the mixture contains more than 95 wt % $MgAl_2O_4$. In addition, the synthesized material contains a small amount of α-BN (hexagonal structure) and Al_2O_3 (Table 2).

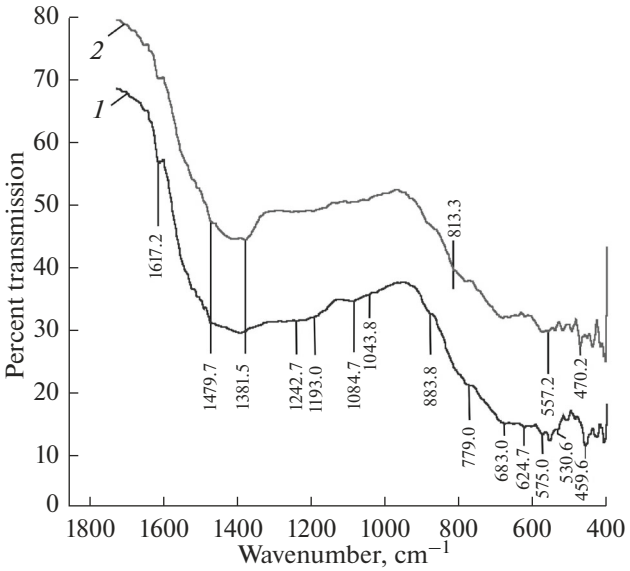

Fig. 6. IR spectra of $MgAl_2O_4$ spinel obtained using the reaction mixtures containing (*1*) 2 and (*2*) 4 wt % B.

Thus, the use of aluminum and boron as reducing agents in the case of rapid heating of the mixture ensures the formation of a material with a large percentage of $MgAl_2O_4$ spinel.

The presence of the BN and Al_2O_3 phases in the composition of the synthesis products is confirmed by IR spectroscopy data (Fig. 6). The spectra of the synthesized $MgAl_2O_4$ spinel contain absorption bands characteristic of tetrahedrally coordinated magnesium, $[MgO_4]$, at 683 cm^{-1} and octahedrally coordinated aluminum, $[AlO_6]$, at 557.2 cm^{-1}. In both cases, there is a peak due to α-Al_2O_3 (459.7 and 470.2 cm^{-1}) [14]. The band at 1617.2 cm^{-1} arises from bending vibrations of adsorbed water, δ(OH) [15].

The synthesis products contain a small amount of tetrahedrally coordinated aluminum, $[AlO_4]$, which shows up as weak features at 1084.7, 1043.8, 779.0, and 624.7 cm^{-1} [16]. $[AlO_4]$ is known to be present in low-temperature alumina polymorphs. In IR spectra of spinels, borates show up as stretching bands of $[BO_3]_3$ planar triangular ions at 1242.7 cm^{-1}. The presence of B_2O_3 in the synthesis products is evidenced by the absorption band at 1479.7 cm^{-1}, which corresponds to asymmetric stretching B–O vibrations in $[BO_3]$ triangles, and by vibrations of the entire $[BO_3]$ triangular groups at 1193.0 and 883.8 cm^{-1} [15, 17].

Aluminoborates containing octahedrally coordinated aluminum, $[AlO_6]$, show up as an absorption band at 575.0 cm^{-1}. The $\nu(B_4–O)$ mode shows up in the range 950–1110 cm^{-1} and overlaps with vibrations of the $[AlO_4]$ groups in this range.

Boron nitride resulting from reaction (7) shows up as vibrations at 1381.5 and 813.3 cm^{-1}, due to the hexagonal polymorph α-BN. Note that, with increasing boron concentration in the starting mixture, the intensity of these bands increases [18].

Figure 7 illustrates the surface morphology of the material synthesized at a high mixture heating rate. The addition of even 2 wt % boron leads to the formation of skeletal crystals, resulting from accelerated growth in a viscous medium. With increasing boron concentration in the starting mixture, the number of such crystals increases. The obtained material is white in color. The spinel crystals range in size from 1 to 20 μm. Skeletal crystals are formed during cooling are typical, for example, of rapidly cooling magmatic melts [19, 20].

With increasing boron concentration in the starting mixture, the maximum synthesis temperature decreases, which is due to the increase in the fraction of the forming B_2O_3 melt. Moreover, a liquid phase can result from the formation of low-melting-point aluminum and magnesium borates. The addition of 2 wt % boron accelerates the formation of spinel compounds in the fabrication of refractories by 15–20 times [1, 22]. In our case, boron in the composition of the starting mixture plays a dual role. On the one hand, it is an energetic additive: boron oxidation is accompanied by the

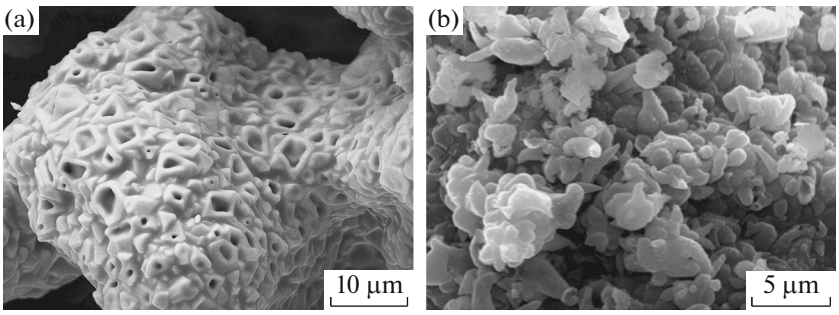

Fig. 7. Micrographs of the synthesis products obtained using the mixture containing 2 wt % B: (a) skeletal $MgAl_2O_4$ particles, (b) hexagonal BN flakes on the surface of $MgAl_2O_4$.

release of a large amount of heat. On the other, the low-melting-point B_2O_3 forming during the boron oxidation process acts as a mineralizer, accelerating spinel synthesis. Boron oxidation with the participation of H_2O(vapor) according to scheme (5) occurs at lower temperatures than does direct boron oxidation. During slow heating, some of the H_2O vaporizes and the fraction of the boron oxide forming by reaction (2) increases.

CONCLUSIONS

The use of aluminum and boron as elemental reducing agents provides conditions for the combustion of a $MgO + Al_2O_3 + Mg(NO_3)_2 \cdot 6H_2O + Al + B$ mixture in the thermal explosion regime. The yield of the desired product, $MgAl_2O_4$ spinel, depends significantly on the sample heating rate. If the mixture is heated at a rate from 7 to 10°C/min, the synthesis product consists of $MgAl_2O_4$ as a major phase, unreacted starting mixture components (MgO, Al_2O_3, and Al), and magnesium borates. A material containing more than 95 wt % $MgAl_2O_4$ spinel has been obtained at a heating rate above 100°C/min. The leading reactions in the SHS process are boron oxidation with oxygen and H_2O vapor. The presence of boron, which forms a low-melting-point oxide during combustion, leads to the formation of a liquid phase, favoring the growth of skeletal $MgAl_2O_4$ spinel crystals 1–10 μm in size. X-ray diffraction and IR spectroscopy data demonstrate that the synthesized material contains small amounts of α-BN and Al_2O_3. Raising the boron content of the starting mixture to above 4 wt % is undesirable because this leads to sintering of the synthesis product, which thus becomes difficult to grind.

FUNDING

This work was supported by the Russian Federation Ministry of Science and Higher Education through the state research targets for the Tomsk Scientific Center, Siberian Branch, Russian Academy of Sciences (theme no. 0365-2019-0005) and the Merzhanov Institute of Structural Macrokinetics and Materials Science, Russian Academy of Sciences (theme no. 45.4).

REFERENCES

1. Khoroshavin, L.B., *Shpinelidnye nanoogneupory* (Spinel Nanorefractories), Yekaterinburg: Ural. Otd. Ross. Akad. Nauk, 2009.
2. Vekinis, G. and Xanthopoulou, G., Hybrid TPS: a novel thermal protection system for atmospheric entry space probes based on SHS-produced MgO/spinel refractories, *Int. J. Self-Propag. High-Temp. Synth.*, 2010, vol. 19, no. 4, pp. 258–275. https://doi.org/10.3103/S1061386210040059
3. Zaychuk, A. and Iovleva, Ju., The study of ceramic pigments of spinel type with the use of slag of aluminothermal production of ferrotitanum, *Chem. Chem. Technol.,* 2013, vol. 7, no. 2, pp. 217–225.
4. Vinnik, I.B., Sirotyuk, M.M., Koval'skii, P.M., and Uvarova, I.V., Refractory and ceramic materials, *Powder Metall. Met. Ceram.,* 1998, vol. 37, nos. 5–6, pp. 287–290.
5. Karanasios, K., Xanthopoulou, G., Vekinis, G., and Zoumpoulakis, L., SHS-produced cobalt–alumina catalysts for dry reforming of methane, *Int. J. Self-Propag. High-Temp. Synth.,* 2014, vol. 23, no. 4, pp. 222–231. https://doi.org/10.3103/S1061386214040037
6. Hui, L., Heng-Yong, W., Yi, C., Rong-Li, S., Jing-Long, B., Ying-Na, W., Jian, L., and Jun-Hong, Z., Synthesis and characterization of $MgAl_2O_4$ spinel nanopowders via nanohydrolytic sol–gel route, *J. Ceram. Soc. Jpn.,* 2017, vol. 125, no. 3, pp. 100–104.
7. Sorokin, V.A., Yanovskii, L.S., Kozlov, V.A., and Surikov, E.V., *Raketno-pryamotochnye dvigateli na tverdykh i pastoobraznykh toplivakh* (Rocket Ramjet Engines Using Solid and Paste Propellants), Moscow: Fizmatlit, 2010.
8. Rabinovich, V.A. and Khavin, Z.Ya., *Kratkii khimicheskii spravochnik* (Brief Chemical Handbook), Leningrad: Khimiya, 1977.
9. Ruzinov, L.P. and Gulyanitskii, B.S., *Ravnovesnye prevrashcheniya metallurgicheskikh reaktsii* (Equilibrium Transformations in Metallurgical Reactions), Moscow: Metallurgiya, 1975.
10. Kovalev, D.Yu. and Ponomarev, V.I., Time-resolved X-ray diffraction in SHS research and related areas: an overview, *Int. J. Self-Propag. High-Temp. Synth.,* 2019, vol. 28, no. 2, pp. 114–123. https://doi.org/10.3103/S1061386219020079
11. Pokhil, P.F., Belyaev, A.F., Frolov, Yu.V., Logachev, V.S., and Korotkov, A.I., *Gorenie poroshkoobraznykh metallov v aktivnykh sredakh* (Combustion of Powder Metals in Active Media), Moscow: Nauka, 1972.
12. Kislyi, P.S., Neronov, V.A., Prikhna, T.A., and Bevza, Yu.V., *Boridy alyuminiya* (Aluminum Borides), Kiev: Naukova Dumka, 1990.
13. Lidin, R.A., Molochko, V.A., and Andreeva, L.L., *Neorganicheskaya khimiya v reaktsiyakh. Spravochnik* (Inorganic Chemistry in Reactions: A Handbook), Moscow: Drofa, 2007.
14. Barabanov, V.F., *Sovremennye fizicheskie metody v geokhimii* (Modern Physical Methods in Geochemistry), Leningrad: Leningrad. Gos. Univ., 1990.
15. Balicheva, T.G. and Lobaneva, O.A., *Elektronnye i kolebatel'nye spektry neorganicheskikh i koordinatsionnykh soedinenii* (Electronic and Vibrational Spectra of Inorganic and Coordination Compounds), Leningrad: Leningrad. Gos. Univ., 1983.
16. Chernyakova, K.V., Vrublevskii, I.A., Ivanovskaya, M.I., and Kotikov, D.A., Impurity–defect structure of anod-

ic alumina produced by double-sided anodization in a tartaric acid solution, *Zh. Prikl. Spektrosk.,* 2012, vol. 79, no. 1, pp. 83–89.

17. Müller, U., *Inorganic Structural Chemistry,* Chichester: Wiley, 2006, 2nd ed.
18. Blank, V.D. and Estrin, E.I., *Fazovye prevrashcheniya v tverdykh telakh pri vysokom davlenii* (High-Pressure Phase Transformations of Solids), Moscow: Fizmatlit, 2011.
19. Shafranovskii, I.I., *Kristally mineralov. Krivogrannye, skeletnye i zernistye formy* (Mineral Crystals: Curved-Face, Skeletal, and Granular Forms), Moscow: Gosgeoltekhizdat, 1961.
20. Ivanov, O.K., Elementary, ideal, and real (equilibrium and nonequilibrium) crystals: systematization, *Ural. Geol. Zh.,* 2012, no. 4, pp. 43–47.
21. Mikhailov, G.G., Makrovets, L.A., and Smirnov, L.A., Thermodynamic modeling of phase equilibria in B_2O_3-containing oxide systems, *Vestn. Yuzhno-Ural. Gos. Univ.,* 2014, vol. 14, no. 4, pp. 11–16.
22. Pishch, I.V., Rotman, T.I., Romanenko, Z.A., and Khainovskaya, E.N., Effect of mineralizers on the physicochemical properties of pigments, *Steklo Keram.,* 1987, no. 4, pp. 23–24.

Translated by O. Tsarev